

# Non-thermal states in models of filaments: a dynamical study

Pierfrancesco Di Cintio<sup>1,2</sup>, Lapo Casetti<sup>2,3,4</sup> & Shamik Gupta<sup>5</sup>

<sup>1</sup> Consiglio Nazionale delle Ricerche, Istituto di Fisica Applicata “Nello Carrara” via Madonna del piano 10, I-50019 Sesto Fiorentino, Italy

<sup>2</sup> INFN - Sezione di Firenze, via G. Sansone 1, I-50019 Sesto Fiorentino, Italy

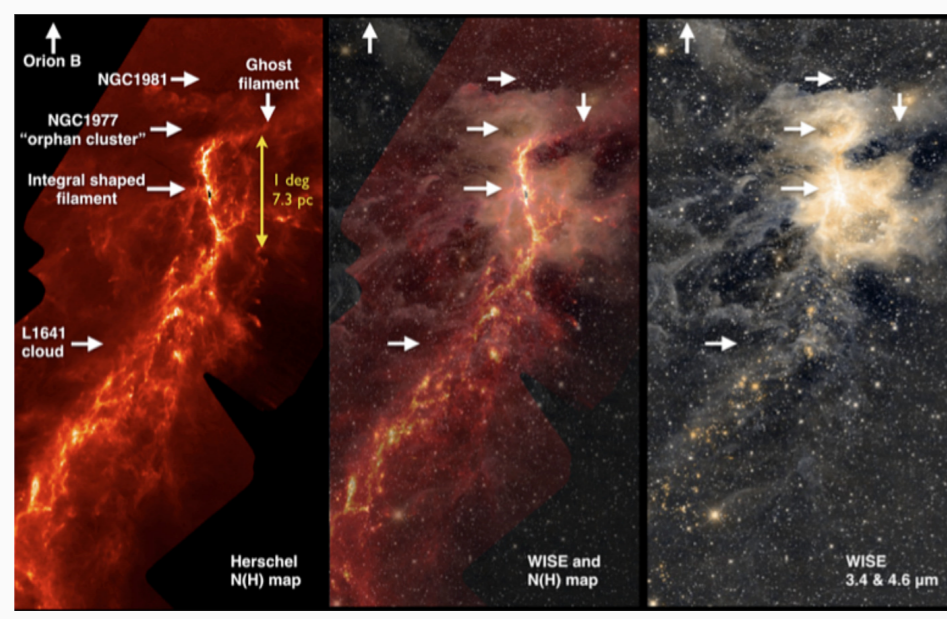
<sup>3</sup> Dipartimento di Fisica e Astronomia and CSDC, Università di Firenze, via G. Sansone 1, I-50019 Sesto Fiorentino, Italy

<sup>4</sup> INAF-Osservatorio Astrofisico di Arcetri, Largo E. Fermi 5, I-50125 Firenze, Italy;

<sup>5</sup> Department of Physics, Ramakrishna Mission Vivekananda University, Belur Math, Dist Howrah 711202 West Bengal, India



## Introduction



- Filaments in galactic molecular clouds are (at least in their initial stages) mainly gravitationally supported structures, that also harbor star-forming cores (Fig. taken from [12]).
- Remarkably, observations suggest that filaments are in non-thermal states [2]; a good description seems to be given by polytropic equations of state  $\rho \propto T^n$  or  $P \propto \rho^\gamma$  [16, 17]. In general it is believed that this is due to the interplay between local turbulence, radiation, and magnetic fields.

To stay simple, we neglect the contribution of magnetic fields. In the fluid picture, the dynamical evolution of self-gravitating filaments is given in terms of mass density  $\rho$ , pressure  $P$ , gravitational potential  $\Phi$  and velocity field  $\mathbf{u}$  by

$$\begin{cases} \partial_t \rho = -\nabla \cdot (\rho \mathbf{u}), \\ \partial_t \mathbf{u} + (\mathbf{u} \cdot \nabla) \mathbf{u} = -\nabla \Phi - \frac{1}{\rho} \nabla P, \\ \Delta \Phi = 4\pi G \rho, \end{cases} \quad (1)$$

that can be closed by assuming an equation of state  $P = P(\rho)$  and whose stationary states can be effectively studied under some simplifying hypotheses, e.g., cylindrical symmetry [16, 17]. We adopt an even simpler model of a filament: assuming our system is infinitely extended along its longitudinal ( $z$ ) axis with perfect cylindrical symmetry, its dynamics is that of a system of infinite straight massive wires, whose mutual interaction is described by a two-dimensional (logarithmic) gravitational potential [13]. Hence, the dynamics in the plane transverse to the  $z$  direction is governed by the Hamiltonian of a two-dimensional system of  $N$  self-gravitating particles,

$$\mathcal{H} = \sum_{i=1}^N \frac{\mathbf{p}_i^2}{2m} + Gm^2 \sum_{i,j=1}^N \log \frac{|\mathbf{r}_i - \mathbf{r}_j|}{r_s}, \quad (2)$$

where  $r_s$  is an arbitrary length scale making the argument of the logarithm dimensionless and the masses  $m$  are related to the total mass per unit length  $M_l$  of the filament by  $m = M_l/N$ . We thus integrated the equations of motion derived from Eq. (2).

## Numerical methods

To begin with we performed direct  $N$ -body simulations of the system (2). In order to effectively explore different initial conditions we were limited to rather small  $N$ 's, of the order of  $10^4$ . To go to larger  $N$ 's we first resorted to standard gravitational particle-in-cell (PIC) methods. The latter however may underestimate the contribution of close encounters that may be relevant. To overcome this problem we adopted a novel method [4, 5] allowing to introduce collisional processes into standard gravitational particle-in-cell code (PIC). The multi-particle collision scheme (MPC), originally introduced in the context of fluid dynamics [8], is based on three simple steps:

- The system of  $N_p$  particles is partitioned in  $N_c$  cells.
- Inside each cell the velocities are stochastically reshuffled in a way that the invariant quantities are preserved (i.e. energy and momentum).
- All particles are propagated freely, or under the effect of an external force if present (In our case the latter is obtained as  $-\nabla \Phi$ , where the potential  $\Phi$  is recovered on a mesh with the standard PIC method and Poisson equation  $\Delta \Phi = 4\pi G \rho$ ).

In a simple two dimensional implementation, at the beginning of each timestep  $\delta t$ , in the cell of indexes  $i, j$  first of all the center of mass velocity is evaluated as

$$\mathbf{u}_{ij} = \frac{1}{n_{ij}} \sum_{k=1}^{n_{ij}} \mathbf{v}_k. \quad (3)$$

Then  $\vartheta_{ij}$  is sampled from a uniform distribution in  $(0, 2\pi)$ . The collision itself is simulated by rotating with probability one-half their relative velocities  $\delta \mathbf{v}_k = \mathbf{v}_k - \mathbf{u}_{ij}$ , as

$$\mathbf{v}'_k = \mathbf{u}_{ij} + \mathcal{R}_{\vartheta_{ij}} \cdot \delta \mathbf{v}_k, \quad (4)$$

where  $\mathcal{R}_{\vartheta_{ij}}$  is the 2D rotation matrix of an angle  $\vartheta_{ij}$ . Such a rotation guarantees the conservation of the total momentum and kinetic energy in the cell:

$$\mathbf{P}_{ij} = \sum_{k=1}^{n_{ij}} m \mathbf{v}_k = \sum_{k=1}^{n_{ij}} m \mathbf{v}'_k, \quad (5)$$

and

$$K_{ij} = \frac{1}{2} \sum_{k=1}^{n_{ij}} m \mathbf{v}_k^2 = \frac{1}{2} \sum_{k=1}^{n_{ij}} m \mathbf{v}'_k^2. \quad (6)$$

Since the effective collisionality may in principle depend on the local state of the system (i.e. temperature and density), the collision move is accepted only if a random probability  $\mathcal{P}_{ij}^*$  sampled from a uniform distribution in  $(0, 1)$  is smaller than the cell dependent collision probability

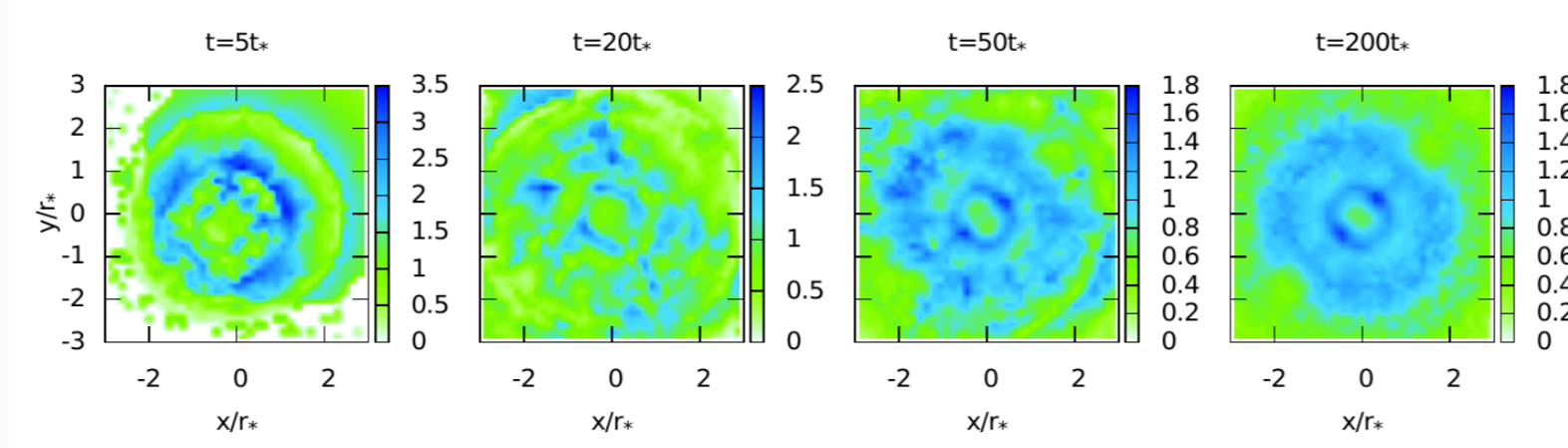
$$\mathcal{P}_{ij} = 1 - \exp[-(v_{ij} \Delta t n_{ij} d_{ij} / \Delta x \Delta y)^2]. \quad (7)$$

In the expression above,  $v_{ij}$  and  $d_{ij}$  are the average velocity and average interparticle distance in the cell, respectively.

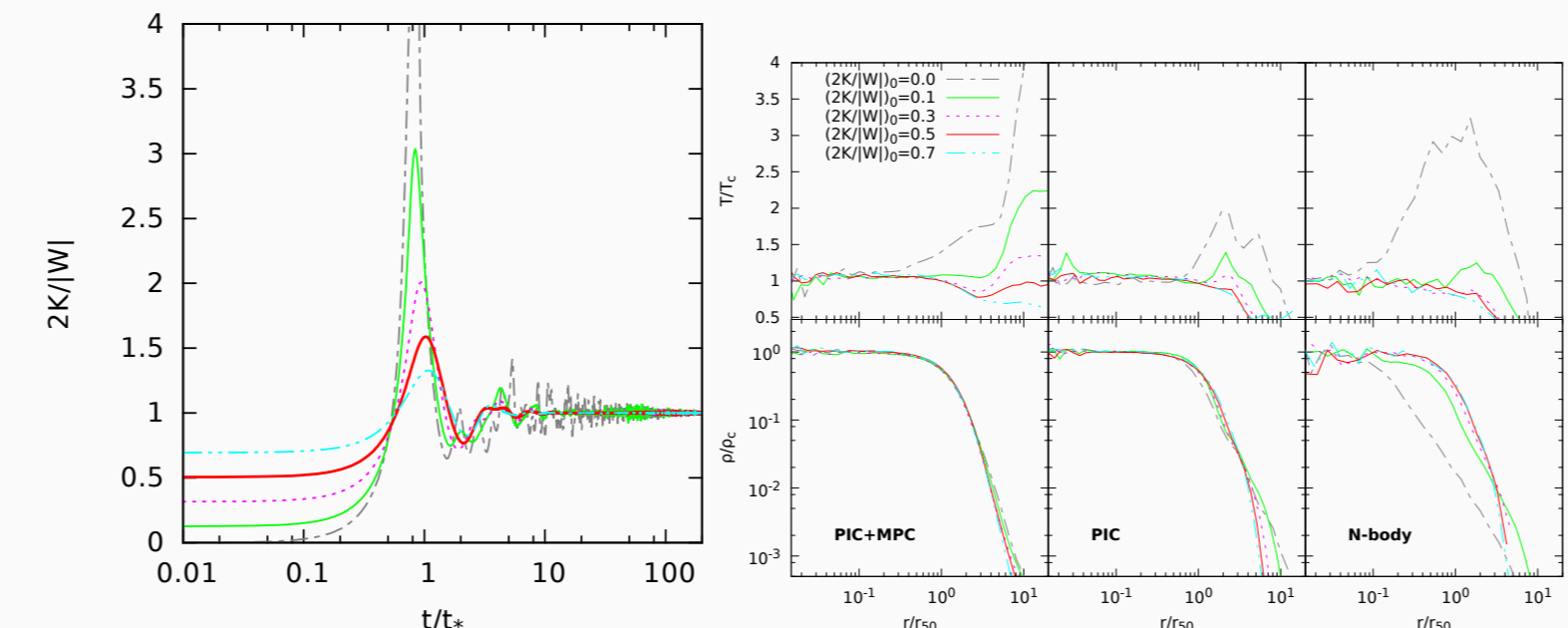
Typically, in our simulations we use  $N \approx 1.5 \times 10^6$  particles on a  $256 \times 256$  cartesian grid.

## Dissipationless collapses

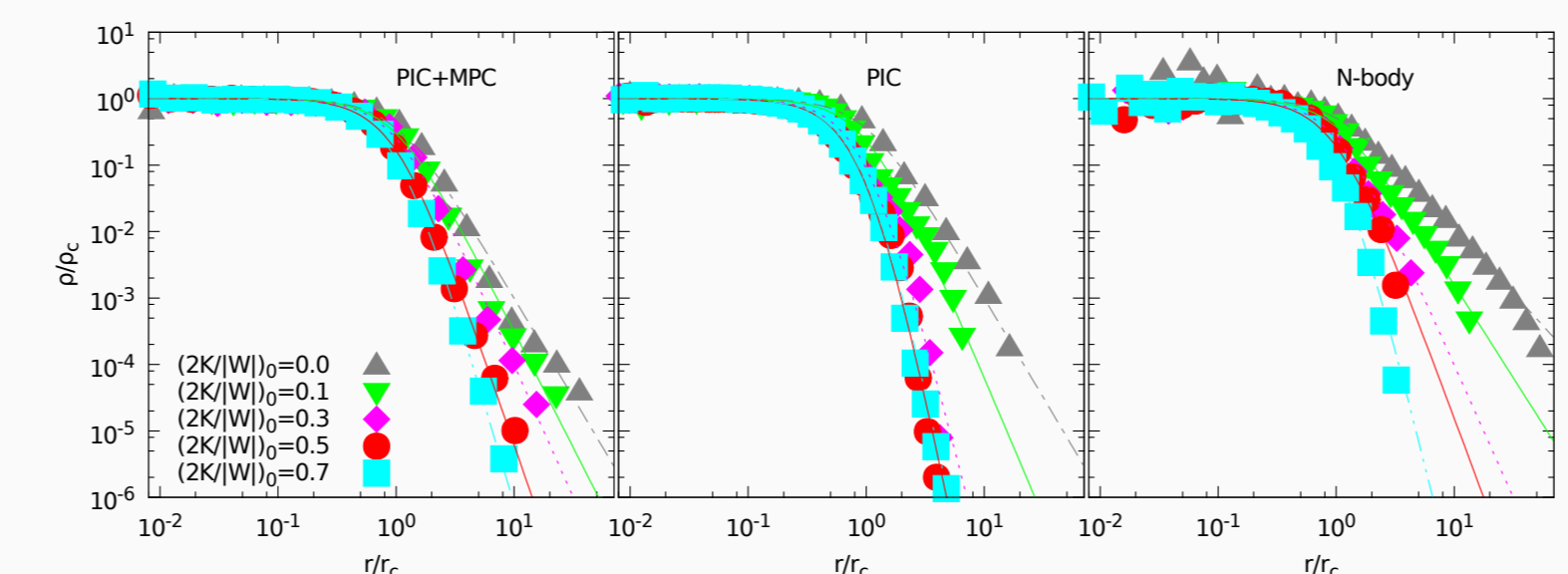
We study the dissipationless collapse [6] of initially cold (i.e.  $2K/|W| < 1$ ), cylindrically symmetric overdensities with Gaussian radial density profile with different mean-square-radius  $r_c$  (in units of half mass radius).



Monitoring the virial ratio, it appears that the systems undergo a violent relaxation phase, the more violent as  $2K/|W|$  is close to 0 at  $t = 0$ . The kinetic temperature profile (i.e. average particle kinetic energy at given radius, see Fig. above) varies strongly throughout the collapse phase.



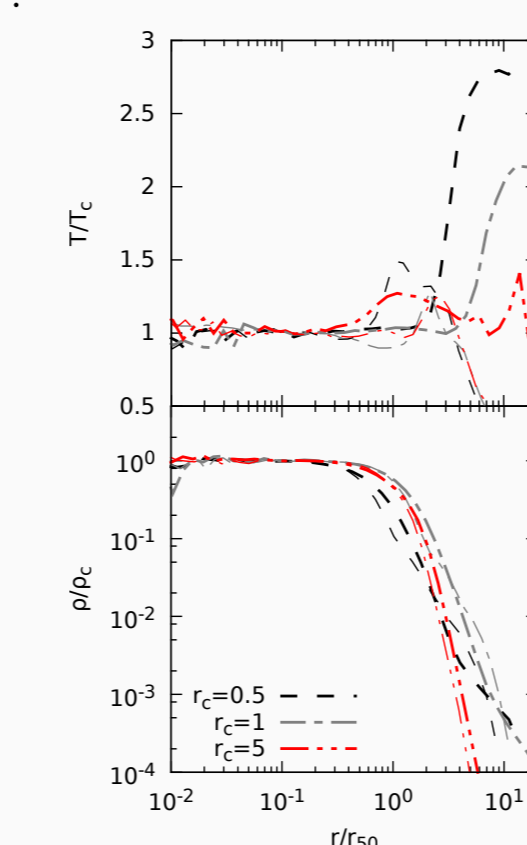
The density and temperature profiles of the final states of PIC-MPC, PIC and  $N$ -body simulations show the same trend with the initial virial ratio. That is, all models have flat almost isothermal cores and power-law tails. Colder systems have a strong temperature-density anticorrelation when collisions are included.



The density profiles are quite well fitted by the empiric law [2]

$$\rho(r) = \frac{\rho_c r_c^\alpha}{(r_c^2 + r^2)^{\alpha/2}}, \quad (8)$$

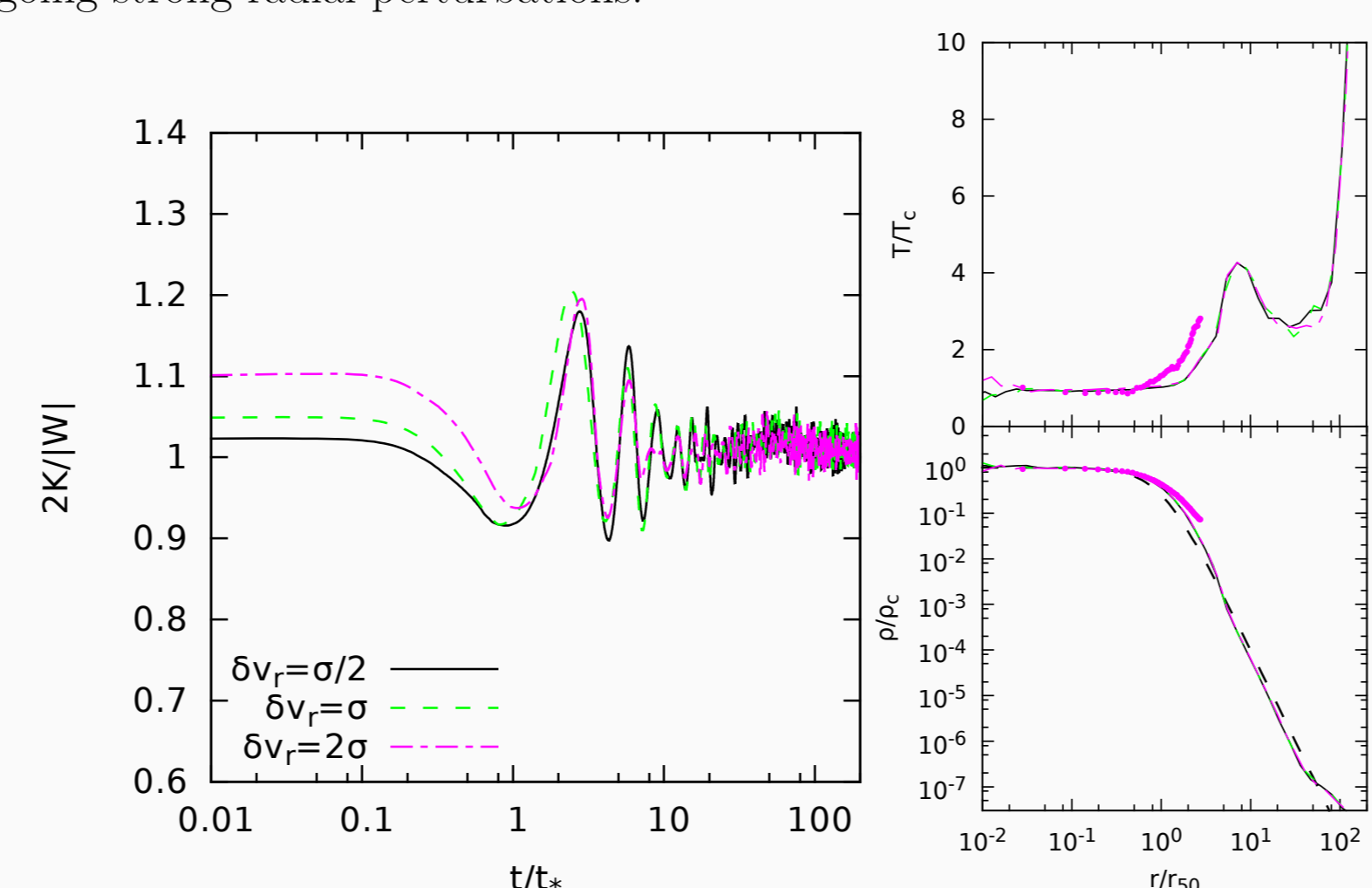
that approximates the solution of Eqs. (1) if the polytropic equation of state is added to the system. Note that for  $\alpha = 4$ , Eq. (8) gives the Ostriker isothermal solution [9]. For the system shown here  $\alpha$  ranges from  $\approx 1.9$  for  $2K/|W| = 0$  to  $\approx 8$  for 0.7.



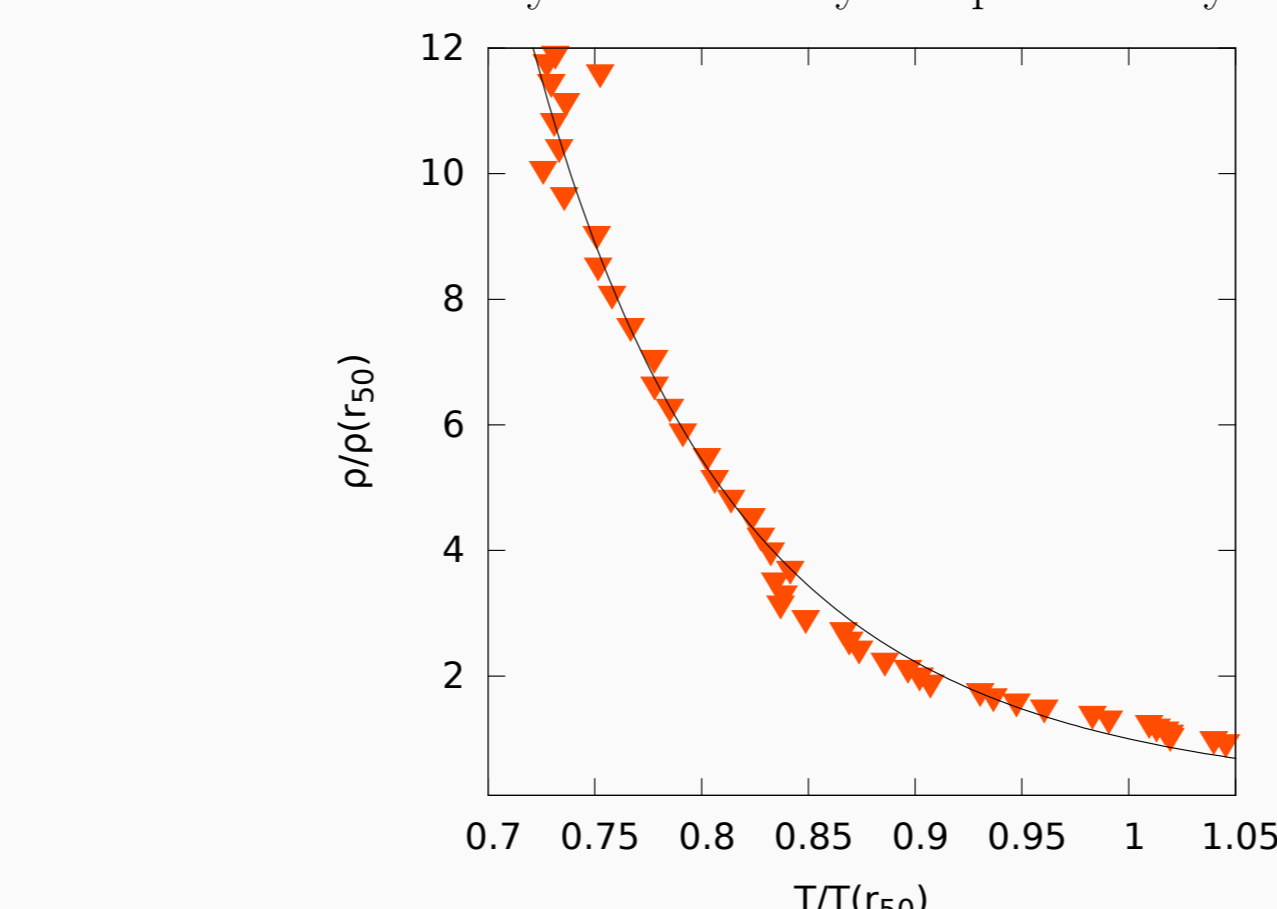
Changing the concentration of the initial condition (i.e. varying the scale radius  $r_c$  at fixed mass) yields different results for fixed initial virial ratio (see fig. on the left). As a general trend, more concentrated system (with or without collisions) have steeper final density profiles and stronger temperature gradients from core to outer regions.

## Perturbed isothermal states

As additional cases (and in the same line of our previous investigation on long-range systems [14, 15]) we also studied the evolution of isothermal Ostriker filaments [9] undergoing strong radial perturbations.



For all cases subjected to a radial compression (or expansion) with a typical velocity larger than roughly  $\sigma/2$ , where  $\sigma$  is the velocity dispersion at equilibrium, the final states are non-thermal with manifest temperature-density anti-correlation. Both PIC-MPC and direct  $N$ -body simulations yield qualitatively similar results.



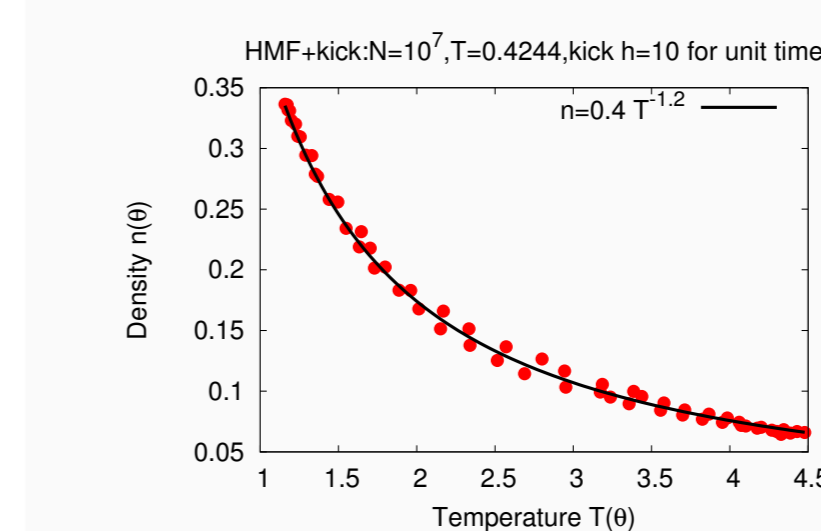
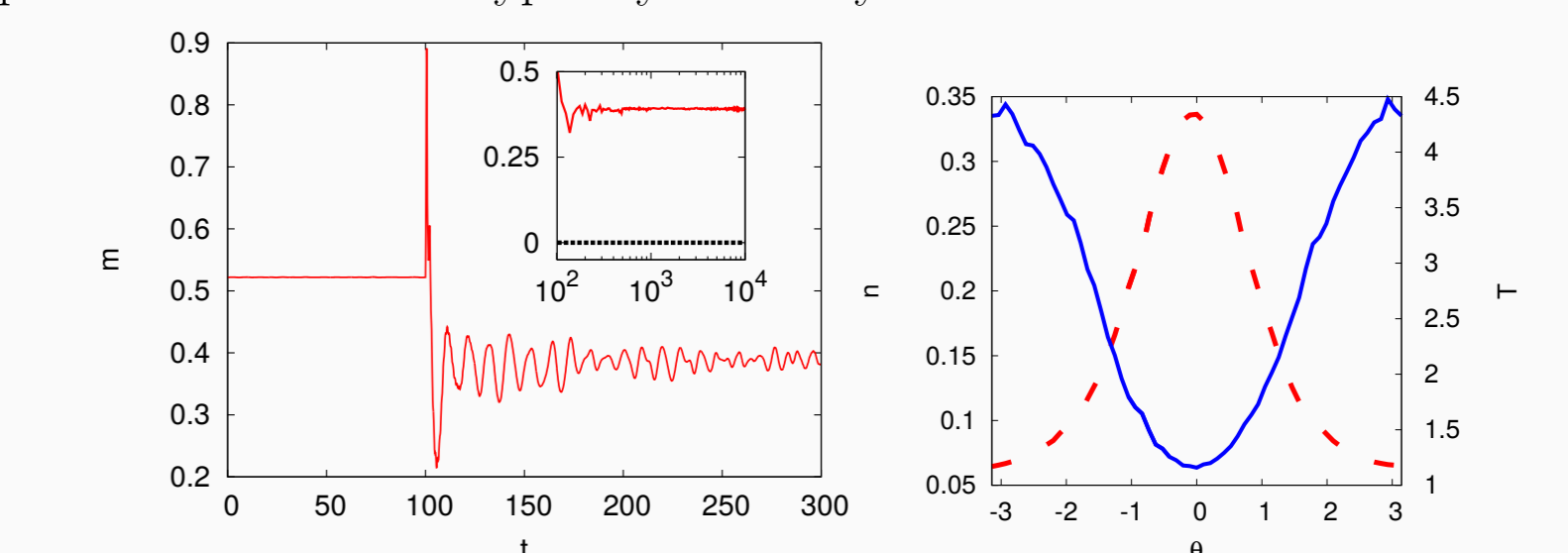
Surprisingly the temperature vs density profiles appear to be well fitted by a polytropic in the region where they are anticorrelated. In general the quality of the fit systematically increases for systems undergoing stronger perturbations.

## Connection with long-range systems

The presence of long-lived non-thermal states is not a feature of self-gravitating systems alone. Any many-body system governed by long-ranged interactions exhibits such quasi-stationary states, provided the number of particles  $N$  is large enough such that collective interactions dominate over binary encounters as far as the dynamics of the single-particle distribution function  $f$  is concerned. Moreover, such states typically exhibit temperature inversion, when arising after the damping of strong collective oscillations [3, 14, 15, 7]. The simplest example is the Hamiltonian Mean Field (HMF) model [1]

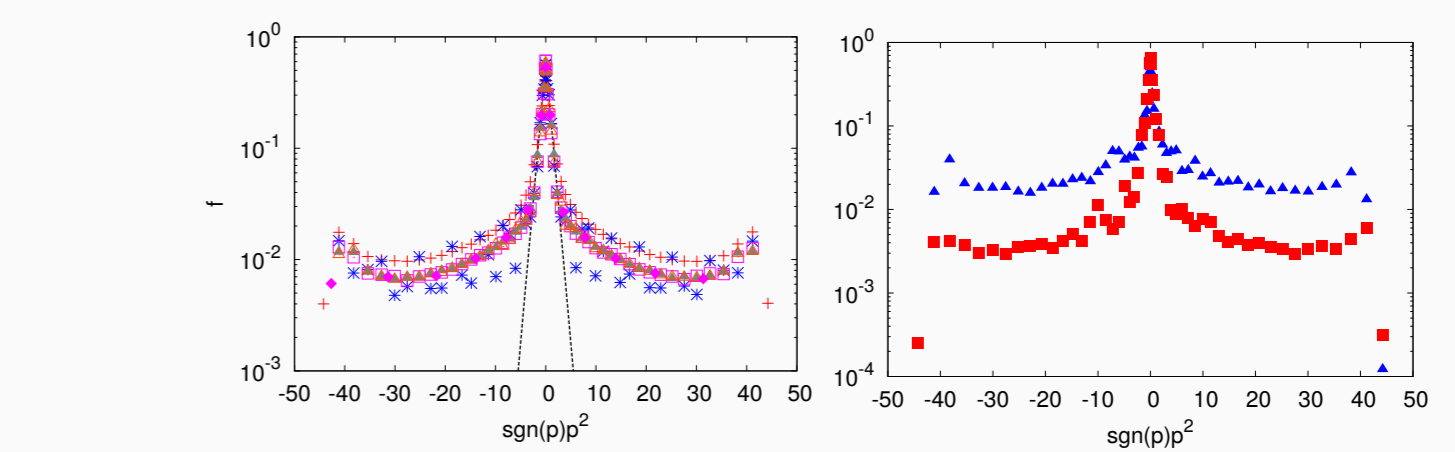
$$\mathcal{H} = \sum_{i=1}^N \frac{p_i^2}{2} + \frac{1}{2N} \sum_{i,j=1}^N [1 - \cos(\vartheta_i - \vartheta_j)]. \quad (9)$$

We start from a thermal equilibrium state and perturb it such as to induce collective interactions in the system, e.g. by applying an external field for a short time [14] or by rapidly quenching a parameter of the Hamiltonian [7], similar to what is done for the model of the filament with a radial perturbation. We monitor the oscillations of the order parameter  $(m_x, m_y) = \frac{1}{N} (\sum_{i=1}^N \cos(\vartheta_i), \sum_{i=1}^N \sin(\vartheta_i))$  and after the oscillations are damped we check the resulting temperature  $T(\vartheta)$  and density  $n(\vartheta)$  profiles.  $T$  and  $n$  are typically markedly anticorrelated.



Remarkably, also for the non-thermal states of the HMF model the relation between  $n$  and  $T$  is nicely fitted by a polytropic when  $n$  and  $T$  are anticorrelated.

A possible mechanism to explain the reason why these non-thermal states exhibit temperature inversion is the fact that during the initial violent relaxation phase the interaction of the particles with the collective oscillations may produce suprathermal tails in the velocity distribution function. In an inhomogeneous system, this may trigger a “velocity filtration” mechanism [10, 11] that effectively broadens the velocity distribution  $f(\mathbf{v})$  when the system is less dense, because only sufficiently fast particles may escape the potential well produced by the central concentration.



## Conclusions

- Dissipationless collapse produces dynamically supported non-thermal end states that look very similar to those observed in filaments, without the need to invoke other mechanisms for their support
- Non-thermal long-lived states with temperature inversion may occur in any long-range-interacting system after the damping of collective oscillations
- Some instances exhibit marked temperature inversion ( $\rho$  and  $T$  are anticorrelated). This is stronger for more concentrated initial conditions and colder initial states as well as for strongly perturbed initially isothermal states
- Both collisions and interactions between particles and collective oscillations may be important to enhance the temperature inversion
- Our model might be too simple yet to allow quantitative comparison with observations; the next step is the inclusion of magnetic fields

## References

- [1] M. Antoni, S. Ruffo *Phys. Rev. E* **52**, 2361 (1995)
- [2] D. Arzoumanian et al., *A&A* **529**, 6 (2011)
- [3] L. Casetti, S. Gupta, *EPJB* **87**, 91 (2014)
- [4] P.F. Di Cintio, R. Livi, H. Bufferand, G. Ciralo, S. Lepri, M.J. Straka, *Phys. Rev. E* **92**, 062108 (2015)
- [5] P.F. Di Cintio, R. Livi, S. Lepri, G. Ciralo, *Phys. Rev. E* **95**, 043203 (2017)
- [6] P.F. Di Cintio, S. Gupta, L. Casetti, *MNRAS* submitted (2017)
- [7] S. Gupta, L. Casetti *New Journal of Physics* **18**, 103051 (2016)
- [8] A. Malevanet, R. Kapral, *J. Chem. Phys.* **110**, 8605 (1999)
- [9] J.P. Ostriker, *ApJ* **140**, 1056 (1964)
- [10] J. Scudder, *ApJ* **398**, 299 (1992)
- [11] J. Scudder, *ApJ* **398**, 319 (1992)
- [12] A.M. Stutz & A. Gould *A&A* **590**, A1 2016
- [13] T.N. Teles, Y. Levin, R. Pakter, F.B. Rizzato, *J. Stat. Mech.* **5**, 05007 (2010)
- [14] T.N. Teles, S. Gupta, P.F. Di Cintio, L. Casetti, *Phys. Rev. E* **92**, 020101 (2015)
- [15] T.N. Teles, S. Gupta, P.F. Di Cintio, L. Casetti, *Phys. Rev. E* **93**, 066102 (2016)
- [16] C. Toci, D. Galli, *MNRAS* **446**, 2110 (2014)
- [17] C. Toci, D. Galli, *MNRAS* **446**, 2118 (2014)